In Vivo Transverse Relaxation and Magnetization Transfer Imaging of Human Thigh Muscles at 3.0 Tesla

Ke Li[1,2], Richard D. Dortch[1,2], Nathan D. Bryant[1,2], Amanda K.W. Buck[1,2], Theodore F. Towse[2,3], Daniel F. Gochberg[1,2], Mark D. Does[1,2], Bruce M. Damon[1,2], and Jane H. Park[4]

[1]Institute of Imaging Science, Vanderbilt University, Nashville, TN, United States, [2]Radiology and Radiological Sciences, Vanderbilt University, Nashville, TN, United States, [3]Physical Medicine and Rehabilitation, Vanderbilt University, Nashville, TN, United States, [4]Molecular Physiology and Biophysics, Vanderbilt University, Nashville, TN, United States

Introduction: Idiopathic inflammatory myopathies (IIM), such as Dermatomyositis (DM) and Polymyositis (PM), are a collection of autoimmune diseases with clinical symptoms of muscle inflammation, fat infiltration/replacement, and atrophy. No direct correlation has been established between the variations of laboratory findings and clinical presentation of IIM. Advances in MRI have yielded a number of contrast-based MRI methods to characterize muscle inflammation and fat infiltration in IIM patients [1]. However, in addition to their physiological sensitivity, these methods are sensitive to the particulars of the acquisition variability. The development of quantitative models for transverse relaxation, magnetization transfer, and diffusion [2,3] may provide the ability to characterize these pathophysiological conditions, independent of the acquisition details. As verified in a small animal model [3], inflammation can be modeled as an increase of the extracellular water component. On the other hand, fibrosis may be modeled by an increase of macromolecular content and can be evaluated using quantitative magnetization transfer (qMT) imaging [3, 4]. Prior to applying these quantitative methods to longitudinal studies such as recovery from injury and treatment response, repeatability has to be established. In this work, a multi-echo sequence for T_2 and a selective inversion recovery (SIR) [4] sequence for qMT were implemented for *in vivo* human thigh muscle imaging, and their repeatability was investigated.

Methods: *Subjects*: Nine healthy subjects (four males) participated in this study. Six subjects have been imaged twice with at an average of 35 days following the first visit. The subjects lay supine in a feet-first position. All subjects have 48-hour restrictions to dietary, exercise, and non-prescription medication. *Data acquisition*: MRI data were acquired on a 3.0-T Philips Achieva MR scanner with a quadrature two-channel body coil for signal excitation and a six-channel SENSE cardiac coil for signal reception. Images were acquired at the center of right thigh in foot-head direction. All images had an in-plane resolution of 2×2 mm^2 and slice thickness of 7 mm. The multi-echo sequence was implemented with composite refocusing pulses and optimized crusher gradients to minimize signal from stimulated echoes [5]. Thirty-two echo data were collected at echo spacing of 10 ms. The SIR data were acquired with a pre-delay of 2.5 s and 16 inversion recovery times ranging from 10 ms to 10 s [6]. To examine the effect of adipose tissue, data were collected with and without fat suppression (FS), a spectral attenuated inversion recovery method and a saturation pulse on the olefinic proton resonance for the multi-echo sequence, and gradient reversal off resonance suppression technique for the SIR sequence. *Data analysis*: The multi-echo data were fitted to a single exponential decay model. The SIR data were fitted to a bi-exponential model [4]. To determine the relaxation parameters of each muscle, regions-of-interests (ROIs) were drawn along the muscle boundaries and pixels affected by partial volume, motion, and flowing artifacts were excluded. For repeatability, Bland-Altman plots of the differences vs. mean values of two measurements validated the repeatability and repeatability coefficients (RC) were calculated. A two-tailed Student's *t*-test was performed and the *p*-values were calculated to compare the two measurements.

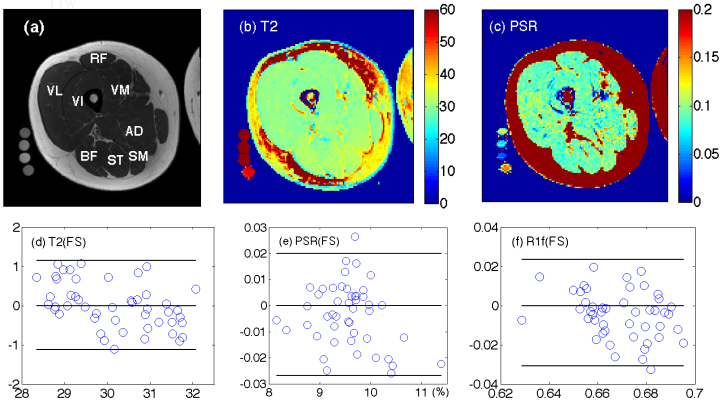

Figure 1, Example data in a male subject: (a) high-resolution anatomical image (b) T2 maps (FS); (c) PSR map (FS), Bland-Altman plots of (d) T_2 (FS), (e) PSR (FS), and (f) R_1 (FS).

Results and Discussion: Figure 1a) shows an example high-resolution anatomical image of a male subject, with eight muscles labeled (RF: rectus femoris; VL: vastus lateralis; VI: vastus intermedius; VM: vastus medialis; AD: adductor magnus; BF: biceps femoris, long head; ST: semitendinosus; SM: semimembranosus). Example T_2 and PSR maps with FS of the same slice are shown in Figure 1b) and 1c). Mean and standard deviations of quantitative relaxation indices, T_2, R_{1f} (the longitudinal relaxation of free water pool), PSR, and k_{mf} (fast exchange rate) of these muscles from all subjects are listed in Table 1. No significant difference in these indices was observed across all muscles and subjects. For qMT studies, PSR values agreed with published with the pulsed technique in [7]. With regard to repeatability, Bland-Altman plots of T_2, PSR (the pool size ratio), and R_{1f} with FS are shown in Figure 1d-f). For the two indices of most interest, T_2 and PSR, their RC values are 1.1 ms and 0.027, respectively. All p-values were found to be greater than 0.05. All these indicate that there is no significant difference between the two measurements. For healthy muscles, no significant differences were observed in the T_2 and PSR values with and without FS applied. This work validates the reliability and repeatability of these methods and their potential application to longitudinal studies. Significant difference is expected in IIM patients [1]. Future work includes improving signal-to-noise-ratio, increase the sequence performance to B1 and B0 inhomogeneity, and application to IIM patient studies with these methods.

Table 1. Determined relaxation indices of thigh muscles at 3.0 T, with FS.

	AD	BF	RF	SM	ST	VI	VL	VM
T2(ms)	30.41(1.00)	30.50(0.89)	29.82(0.75)	30.66(1.14)	29.78(0.96)	30.45(0.78)	30.81(0.84)	30.54(0.88)
$R_{1f}(s^{-1})$	0.67(0.01)	0.67(0.01)	0.66(0.01)	0.66(0.02)	0.66(0.01)	0.67(0.01)	0.67(0.01)	0.67(0.01)
PSR(%)	9.36(0.73)	9.00(0.70)	9.11(0.61)	9.88(0.81)	9.43(0.72)	8.83(0.92)	9.32(1.07)	8.84(0.76)
$k_{mf}(s^{-1})$	40.90(7.08)	36.98(7.05)	45.64(7.81)	38.49(10.48)	36.15(8.34)	40.84(5.29)	41.92(6.98)	44.00(4.85)

References: [1] Park JH et al, *Radiology*, 177:473 (1990); [2] Louie EA et al, MRM, 61:560 (2009); [3] Bryant ND et al, *Proc ISMRM 20*:1442(2012); [4] Gochberg DF et al, *MRM*, 57:437(2007); [5] Poon CS et al, *JMRI*, 2:541(1992); [6] Dortch RD et al, *MRM*, 66:1346 (2011); [7] Sinclair CD et al, *MRM*, 64:1739(2010).